Thermoelastic Small-Amplitude Wave Propagation in Nonlinear Elastic Multilayers

MASSIMILIANO GEI
DAVIDE BIGONI
GIULIA FRANCESCHINI
Dipartimento di Ingegneria Meccanica e Strutturale, Università di Trento, Via Mesiano 77, I-38050 Trento, Italy

(Received 4 February 2003; accepted 27 February 2003)

Dedicated to Prof. Raymond W. Ogden

Abstract: A framework for thermoelastic analysis of wave propagation in multilaminated structures is given. The elastic material is subject to an arbitrary, homogeneous deformation and to a condition of uniform temperature. Small-amplitude vibrations are analyzed starting from this state, in a fully coupled thermomechanical formulation.

Key Words: Thermoelasticity, Nonlinear Elasticity, Dynamics.

1. INTRODUCTION

Due to their excellent mechanical performances, composite materials and structures have attracted an intense research effort in recent years. Layered elastic structures are employed in a broad range of applications, including laminated timber structures in civil engineering, sandwich panels in aircraft, submarine coatings, integrated circuits, thin film deposition in semiconductor devices.

These structures are usually subject to a number of static and dynamic loading processes, including temperature changes. Due to the fact that the layers possess different mechanical and thermal properties, temperature changes can introduce stresses that may lead to failure. For instance, multilayer capacitors often consist of a one hundred alternate layers of electrodes and dielectric ceramics, sandwiched between two ceramic cover layers [1]. Consequently to the thermomechanical mismatch between constituents, these devices are generally subject to residual stresses, so that the brittle dielectric layer may crack or the electrode/dielectric interface may debond, leading to failure of the system.

Analysis of vibration and instability in the above-mentioned situations, where both pre-stress and thermal effects play a role, has an obvious meaning for design purposes. As a consequence, a number of mechanical models were formulated at different levels of sophistication [2, 3, 4, 5]. All these models are however based on approximate plate

 DOI: 10.1177/1081286504038675

theories, while our interest here is to develop a framework for the analysis of small-amplitude waves superimposed upon an arbitrarily large and uniform deformation of a nonlinear elastic material. This framework was thoroughly analyzed in the isothermal case for quasi-static deformation [6, 7, 8, 9, 10, 11], while isothermal vibrations were considered mainly by Ogden and co-Workers [12, 13, 14].

Within the framework of modified entropic theory, layered and compressible hyperelastic, nonlinear materials are considered in this article, deformed an arbitrary amount with deformations having principal Eulerian axes aligned parallel and orthogonal to the layers. Temperature is assumed uniform in this configuration and equal in all layers. Thermoelastic, plane strain, and small-amplitude waves are analyzed from this state, in a fully coupled formulation. Within the analyzed range of parameters, it is shown that the coupling terms, yielding complex propagation velocities, introduce a small dispersion effect. However, temperature and pre-strain result to play an important role in determining the propagation characteristics of the structures.

2. THERMOELASTIC CONSTITUTIVE EQUATIONS

The formulation of constitutive equations is based upon the deformation gradient $\mathbf{F}$ and the absolute temperature Θ which are taken to be the two thermodynamic independent variables. The Helmholtz free energy $\psi(\mathbf{F}, \Theta)$ is then introduced so that the first Piola-Kirchhoff stress tensor $\mathbf{S}$ and the entropy η are given by the following constitutive equations [15, 16, 17]

$$\mathbf{S} = \frac{\partial \psi(\mathbf{F}, \Theta)}{\partial \mathbf{F}}, \quad \eta = -\frac{\partial \psi(\mathbf{F}, \Theta)}{\partial \Theta}, \tag{1}$$

while the specific internal energy e follows from the relationship

$$e = \psi + \Theta \eta. \tag{2}$$

It has been shown (see, for instance, [17]) that the free energy for a thermoelastic material may take the form

$$\psi(\mathbf{F}, \Theta) = \psi_0(\mathbf{F}) \frac{\Theta}{\Theta_0} - e_0(\mathbf{F}) \frac{\Theta - \Theta_0}{\Theta_0} + \int_{\Theta_0}^{\Theta} c(\mathbf{F}, \tilde{\Theta}) \frac{(\tilde{\Theta} - \Theta)}{\tilde{\Theta}} d\tilde{\Theta}, \tag{3}$$

where $\psi_0(\mathbf{F}) = \psi(\mathbf{F}, \Theta_0)$ is the isothermal free energy at the reference temperature Θ_0, $e_0(\mathbf{F}) = e(\mathbf{F}, \Theta_0)$ and the heat capacity at constant strain $c(\mathbf{F}, \Theta)$ is given by $c = \partial e(\mathbf{F}, \Theta)/\partial \Theta$.

In order to study the behaviour of thermoelastic rubberlike materials a free energy obeying a class of modified entropic theories proposed by Chadwick [17, 18] is employed, thus allowing the internal energy e to be split into two contributions, one depending on the deformation through the volume ratio $J = \det \mathbf{F}$, the other depending on the temperature, namely $e = e_0(J) + e_\Theta(\Theta)$. As a consequence $c = c(\Theta)$ and (3) takes the form

$$\psi(\mathbf{F}, \Theta) = \psi_0(\mathbf{F}) \frac{\Theta}{\Theta_0} - e_0(J) \frac{\Theta - \Theta_0}{\Theta_0} + \int_{\Theta_0}^{\Theta} c(\tilde{\Theta}) \frac{(\tilde{\Theta} - \Theta)}{\tilde{\Theta}} d\tilde{\Theta}. \tag{4}$$

As a specific form of the isothermal free energy ψ_0, the isotropic, compressible, two-parameters neo-Hookean elasticity is considered, defined in terms of principal stretches λ_1, λ_2, λ_3 as [19]

$$\psi_0(\lambda_1,\lambda_2,\lambda_3) = \frac{\lambda_0}{2}(\lambda_1\lambda_2\lambda_3 - 1)^2 + \frac{\mu_0}{2}\left[\lambda_1^2+\lambda_2^2+\lambda_3^2 - 3 - 2\ln(\lambda_1\lambda_2\lambda_3)\right], \quad (5)$$

where λ_0 and μ_0 represent the Lamé constant in an unstressed configuration at the reference temperature Θ_0. In addition, we employ the following relation proposed by Chadwick [17] for the internal energy term,

$$e_0(J)/\Theta_0 = 3\alpha_0\kappa_0 h(J), \quad (6)$$

where α_0 is the linear thermal expansion coefficient, $\kappa_0 = \lambda_0 + 2\mu_0/3$ is the elastic bulk modulus in the unstressed configuration at $\Theta = \Theta_0$, and

$$h(J) = \gamma^{-1}(J^\gamma - 1), \quad \gamma > 1. \quad (7)$$

In the case which c is constant, the free energy (4) becomes

$$\begin{aligned} \psi &= \frac{1}{2}\left[\lambda_0(J-1)^2 + \mu_0(\lambda_1^2+\lambda_2^2+\lambda_3^2-3-2\ln J)\right]\frac{\Theta}{\Theta_0} \\ &- 3\alpha_0\kappa_0\gamma^{-1}(J^\gamma-1)(\Theta-\Theta_0) + c[\Theta-\Theta_0-\Theta\ln(\Theta/\Theta_0)]. \end{aligned} \quad (8)$$

The propagation of small-amplitude waves is studied by means of incremental equations. The constitutive equations of incremental thermoelasticity are now formulated on the basis of the nonlinear, finite equations (1).

Denoting with δ first-order incremental quantities, we get

$$\delta\mathbf{S} = \mathbb{C}_0^\Theta\delta\mathbf{F} + \mathbf{M}_0\delta\Theta, \quad (9)$$

where

$$\mathbb{C}_0^\Theta = \frac{\partial\mathbf{S}(\mathbf{F},\Theta)}{\partial\mathbf{F}} = \frac{\partial^2\psi(\mathbf{F},\Theta)}{\partial\mathbf{F}^2}, \quad \mathbf{M}_0 = \frac{\partial\mathbf{S}(\mathbf{F},\Theta)}{\partial\Theta} = \frac{\partial^2\psi(\mathbf{F},\Theta)}{\partial\Theta\partial\mathbf{F}}, \quad (10)$$

are the isothermal elastic tensor and the stress-temperature constitutive tensor, respectively. An updated Lagrangian formulation of the boundary-value problem will be employed. Then, on introducing the pertinent stress $\boldsymbol{\Sigma}$ and deformation gradient $\boldsymbol{\Gamma}$ increments [20]

$$J\boldsymbol{\Sigma} = \delta\mathbf{S}\mathbf{F}^T, \quad \boldsymbol{\Gamma} = (\delta\mathbf{F})\mathbf{F}^{-1}, \quad (11)$$

(where the superscript T denotes the transpose) the constitutive equation (9) becomes

$$\boldsymbol{\Sigma} = \mathbb{C}^\Theta\boldsymbol{\Gamma} + \mathbf{M}\delta\Theta. \quad (12)$$

The fourth-order tensor $\mathbb{C}^{\Theta}$ is given by

$$J\mathbb{C}^{\Theta} = (\mathbf{I} \boxtimes \mathbf{F})\, \mathbb{C}_0^{\Theta} \left(\mathbf{I} \boxtimes \mathbf{F}^T\right), \tag{13}$$

where $\mathbf{I}$ denotes the identity tensor and the following tensorial product between three arbitrary second-order tensors $\mathbf{A}$, $\mathbf{B}$, $\mathbf{C}$, has been introduced

$$(\mathbf{A} \boxtimes \mathbf{B})\, \mathbf{C} = \mathbf{A}\mathbf{C}\mathbf{B}^T. \tag{14}$$

The updated stress-temperature tensor $\mathbf{M}$ appearing in eqn. (11) turns out to be given by

$$\mathbf{M} = J^{-1}\mathbf{M}_0\mathbf{F}^T = \frac{\partial \mathbf{T}\,(\mathbf{F}, \Theta)}{\partial \Theta}, \tag{15}$$

where

$$\mathbf{T} = J^{-1}\mathbf{S}\mathbf{F}^T \tag{16}$$

denotes the Cauchy stress tensor.

For an isotropic material the non-null components of the isothermal elastic tensor $\mathbb{C}^{\Theta}$ are [20]

$$\begin{aligned} JC^{\Theta}_{iijj} &= \lambda_i\lambda_j \frac{\partial^2 \psi}{\partial\lambda_i\partial\lambda_j}, \\ JC^{\Theta}_{ijij} &= \lambda_j^2 \frac{\lambda_j \frac{\partial\psi}{\partial\lambda_j} - \lambda_i \frac{\partial\psi}{\partial\lambda_i}}{\lambda_j^2 - \lambda_i^2}, \quad i \neq j,\ \lambda_i \neq \lambda_j, \\ JC^{\Theta}_{ijji} &= JC^{\Theta}_{ijij} - \lambda_j \frac{\partial\psi}{\partial\lambda_j}, \qquad i \neq j. \end{aligned} \tag{17}$$

For the free energy (8) and a plane-strain condition, where $\lambda_3 = 1$, the in-plane components of $\mathbb{C}^{\Theta}$ different from zero result to be

$$C_1 = C^{\Theta}_{1111} = \mu_0 \frac{\Theta}{\Theta_0} \frac{1+\lambda_1^2}{J} + \lambda_0 \frac{\Theta}{\Theta_0} J - 3\alpha_0\kappa_0(\Theta - \Theta_0)(\gamma - 1)J^{\gamma-1}, \tag{18}$$

$$C_2 = C^{\Theta}_{2222} = \mu_0 \frac{\Theta}{\Theta_0} \frac{1+\lambda_2^2}{J} + \lambda_0 \frac{\Theta}{\Theta_0} J - 3\alpha_0\kappa_0(\Theta - \Theta_0)(\gamma - 1)J^{\gamma-1}, \tag{19}$$

$$C_3 = C^{\Theta}_{1122} = C^{\Theta}_{2211} = \lambda_0 \frac{\Theta}{\Theta_0}(2J - 1) - 3\alpha_0\kappa_0(\Theta - \Theta_0)\gamma J^{\gamma-1}, \tag{20}$$

$$C_4 = C^{\Theta}_{1221} = C^{\Theta}_{2112} = \mu_0 \frac{\Theta}{\Theta_0} \frac{1}{J} - \lambda_0 \frac{\Theta}{\Theta_0}(J - 1) + 3\alpha_0\kappa_0(\Theta - \Theta_0)J^{\gamma-1}, \tag{21}$$

$$C_5 = C^{\Theta}_{1212} = \mu_0 \frac{\Theta}{\Theta_0} \frac{\lambda_2^2}{J}, \tag{22}$$

$$C_6 = C^{\Theta}_{2121} = \mu_0 \frac{\Theta}{\Theta_0} \frac{\lambda_1^2}{J}. \tag{23}$$

In the Eulerian reference system, the Cauchy stress is diagonal with components

$$T_i = J^{-1} \lambda_i \frac{\partial \psi}{\partial \lambda_i}, \tag{24}$$

and the stress-temperature tensor $\mathbf{M}$ has also a diagonal form

$$M_i = \frac{\partial T_i}{\partial \Theta}, \tag{25}$$

so that

$$M_1 = \mu_0 \frac{\lambda_1^2 - 1}{J} \frac{1}{\Theta_0} + \lambda_0 (J-1) \frac{1}{\Theta_0} - 3\alpha_0 \kappa_0 J^{\gamma - 1}, \tag{26}$$

$$M_2 = \mu_0 \frac{\lambda_2^2 - 1}{J} \frac{1}{\Theta_0} + \lambda_0 (J-1) \frac{1}{\Theta_0} - 3\alpha_0 \kappa_0 J^{\gamma - 1}. \tag{27}$$

It should be noted that in the case when the pre-strain is null, $\lambda_1 = \lambda_2 = \lambda_3 = 1$, the constitutive equation (12) reduces to

$$\delta \mathbf{T} = \tilde{\lambda} \operatorname{div} \mathbf{u} \mathbf{I} + \tilde{\mu} \left(\nabla \mathbf{u} + \nabla \mathbf{u}^T \right) - 3\alpha_0 \kappa_0 \, \delta \Theta \, \mathbf{I}, \tag{28}$$

where $\delta \mathbf{T}$ and $\mathbf{u}$ denote increments of Cauchy stress and displacement, respectively, div and ∇ are the divergence and gradient operators and

$$\tilde{\lambda} = \lambda_0 \frac{\Theta}{\Theta_0} - 3\gamma \alpha_0 \kappa_0 (\Theta - \Theta_0), \quad \tilde{\mu} = \mu_0 \frac{\Theta}{\Theta_0} + \frac{3}{2} \alpha_0 \kappa_0 (\Theta - \Theta_0). \tag{29}$$

It should be noted that $\tilde{\lambda}$ and $\tilde{\mu}$ are independent of the incremental quantities, so that the form (28) of the constitutive law represents the well-known equations of infinitesimal thermoelasticity [15].

3. THE LAYERED STRUCTURE

An elastic structure made up of different isotropic thermoelastic layers is considered, obeying constitutive laws (1) and (8) and subject to uniform (arbitrary large) deformation and temperature. In the reference configuration, layers are rectangular strips of infinite length in the direction 1 and 3 with material points defined by the coordinates (for the h-th layer)

$$-\infty < x_i^0 < +\infty \quad (i = 1, 3), \qquad l^0_{h,min} < x_2^0 < l^0_{h,max}. \tag{30}$$

The layers are subject to a uniform stretch, so that the current configuration is defined by

$$-\infty < x_i < +\infty \quad (i = 1, 3), \qquad l_{h,min} < x_2 < l_{h,max}\,, \tag{31}$$

where $x_i = \lambda_i x_i^0$ $(i = 1, 3)$, $x_2 = l_{h,min} + \lambda_2(x_2^0 - l_{h,min}^0)$ at a given temperature Θ. As a consequence, eqns. (17) and (24) allow us to evaluate the current elastic tensor, the Cauchy stress and stress-temperature tensor.

Starting from the above configuration, the propagation of small-amplitude mechanical disturbances are analyzed. These must satisfy:

- the incremental equations of motion in the absence of body forces

$$\mathrm{div}\,\boldsymbol{\Sigma} = \rho\ddot{\mathbf{u}}, \tag{32}$$

where a dot means material time derivative, ρ is the mass density and $\mathbf{u}$ the incremental displacement. Tensor $\boldsymbol{\Sigma}$ is specified by eqn. (12) in the form

$$\boldsymbol{\Sigma} = \mathbb{C}^{\Theta}\nabla\mathbf{u} + \mathbf{M}\theta, \tag{33}$$

where $\theta = \delta\Theta$ is the increment of temperature;

- the local conservation of energy in the absence of heat sources

$$\bar{c}\,\dot{\theta} = -\mathrm{div}\mathbf{q} + \Theta\mathbf{M}\cdot\nabla\dot{\mathbf{u}}, \tag{34}$$

where $\bar{c} = c/J$, $\mathbf{q}$ is the heat flux, that can be expressed in terms of θ through the Fourier law

$$\mathbf{q} = -K\nabla\theta,$$

where K is the thermal conductivity;

- incremental plane strain constraint in direction 3

$$u_3 = 0,\ \Sigma_{13} = \Sigma_{31} = \Sigma_{23} = \Sigma_{32} = 0; \tag{35}$$

- the mechanical boundary conditions
  - at a boundary subject to dead load:

$$\Sigma_{22} = 0, \quad \Sigma_{12} = 0; \tag{36}$$

  - at an interface between two layers denoted by $^+$ and $^-$:

$$\Sigma_{22}^+ = \Sigma_{22}^-, \quad \Sigma_{12}^+ = \Sigma_{12}^-, \quad \mathbf{u}^+ = \mathbf{u}^-; \tag{37}$$

- the thermal boundary conditions
  - at any external boundary:

$$\text{either adiabatic } \frac{\partial\theta}{\partial x_2} = 0, \text{ or prescribed temperature } \theta = \bar{\theta}\,; \tag{38}$$

– at an interface between two layers denoted by $^+$ and $^-$:

$$\theta^+ = \theta^-, \quad K^+ \frac{\partial \theta^+}{\partial x_2} = K^- \frac{\partial \theta^-}{\partial x_2}. \tag{39}$$

Solutions to the above problem are sought in the form of small-amplitude waves propagating in the direction 1

$$\{u_1, u_2, \theta\} = \{\phi_1(x_2), \phi_2(x_2), \phi_\theta(x_2)\} e^{ik(x_1 - vt)}, \tag{40}$$

where k is the wavenumber and v the velocity, both complex valued. Functions $\phi_1(x_2), \phi_2(x_2), \phi_\theta(x_2)$ can be determined by substituting (40) into the equations of motion (32) and the local conservation of energy (34). This gives a system of three second-order ODEs which admits the solution

$$\{\phi_1(x_2), \phi_2(x_2), \phi_\theta(x_2)\} = \sum_{j=1}^{3} \{A_j, B_j, Z_j\} e^{s_j k x_2} + \{A_{j+3}, B_{j+3}, Z_{j+3}\} e^{-s_j k x_2}, \tag{41}$$

where A_j, B_j, Z_j $(j = 1, ..., 6)$ are unknown constants. The six complex roots $s_1 = -s_4$, $s_2 = -s_5$, and $s_3 = -s_6$ are the solutions of the characteristic equation [21]

$$\begin{aligned} &\{\bar{C}_5 s^2 - (1 + \bar{M}_1^2 \Xi) + \rho v^2/C_1\}\{(\bar{C}_2 + \bar{M}_2^2 \Xi)s^2 - \bar{C}_6 + \rho v^2/C_1\} \\ &+\{(\bar{C}_3 + \bar{C}_4) + \bar{M}_1 \bar{M}_2 \Xi\}^2 s^2 + i(1 - s^2) Q C_1/(\rho v^2) \times \\ &\times\{(\bar{C}_5 s^2 - 1 + \rho v^2/C_1)(\bar{C}_2 s^2 - \bar{C}_6 + \rho v^2/C_1) + (\bar{C}_3 + \bar{C}_4)^2 s^2\} = 0, \end{aligned} \tag{42}$$

where $\bar{C}_j = C_j/C_1$, $\bar{M}_j = M_j/\bar{c}$, $\Xi = \Theta \bar{c}/C_1$ and $Q = kvK\rho/(C_1 \bar{c})$.

Note that for $s = 0$ waves are independent of the tranversal direction and eqn. (42) gives

$$(C_6 - \rho v^2)\left[(C_1 - \rho v^2)(kK - i\bar{c}v) - ivM_1^2 \Theta\right] = 0,$$

yielding the propagation conditions of shear and longitudinal body waves.

Substitution of (40)–(41) into (32) yields two relations which allow us to express the constants B_j, Z_j $(j = 1, ..., 6)$ in terms of A_j $(j = 1, ..., 6)$, namely

$$B_j = f(s_j) A_j, \quad B_{j+3} = -f(s_j) A_{j+3} \quad (j = 1, 2, 3), \tag{43}$$

$$Z_j = g(s_j) A_j, \quad Z_{j+3} = g(s_j) A_{j+3} \quad (j = 1, 2, 3), \tag{44}$$

where

$$f(s_j) = -s_j \frac{i\bar{M}_2(\bar{C}_5 s_j^2 + \rho v^2/C_1 - 1) + i\bar{M}_1(\bar{C}_3 + \bar{C}_4)}{\bar{M}_1(\bar{C}_2 s_j^2 + \rho v^2/C_1 - \bar{C}_6) - \bar{M}_2 s_j^2(\bar{C}_3 + \bar{C}_4)}, \tag{45}$$

and

$$g(s_j) = iQ\frac{C_1^2}{\rho v K}\frac{(\bar{C}_3+\bar{C}_4)^2 s_j^2 + (\bar{C}_5 s_j^2 + \rho v^2/C_1 - 1)(\bar{C}_2 s_j^2 + \rho v^2/C_1 - \bar{C}_6)}{\bar{M}_1(\bar{C}_2 s_j^2 + \rho v^2/C_1 - \bar{C}_6) - \bar{M}_2 s_j^2(\bar{C}_3+\bar{C}_4)}. \tag{46}$$

In conclusion, the displacement and the temperature fields associated with the travelling wave are expressible in the form

$$\{u_1, u_2, \theta\} = \sum_{j=1}^{3} \left[\{1, f(s_j), g(s_j)\}A_j e^{s_j kx_2} + \{1, -f(s_j), g(s_j)\}A_{j+3} e^{-s_j kx_2}\right] e^{ik(x_1 - vt)}. \tag{47}$$

Once the form of solution (47) is substituted into the boundary conditions (36)–(39), an eigenvalue problem for the complex propagation velocity v is obtained, which can be solved numerically. Finally, for each propagation velocity, the same eigenvalue problem provides the propagation amplitudes A_j $(j = 1, ..., 6)$ unless an arbitrary constant, and finally B_j and Z_j from eqns. (43)–(44).

4. RESULTS

Results relative to simple geometries are presented in the following. Uniaxial tensile and compressive stress states have been analyzed for simplicity, in globally adiabatic conditions, eqn. $(38)_1$. In particular, a longitudinal stretch λ_1 and a constant temperature Θ have been imposed uniformly for the whole multilaminated structure. The stretch in the transversal direction λ_2 has been calculated by imposing the vanishing of the transversal stress

$$T_2 = \frac{1}{J}\lambda_2 \frac{\partial \psi}{\partial \lambda_2} = 0, \tag{48}$$

thus obtaining a relationship determining λ_2

$$\mu_0 \frac{\Theta}{\Theta_0}\left(\frac{\lambda_2}{\lambda_1} - \frac{1}{\lambda_1 \lambda_2}\right) + \lambda_0 \frac{\Theta}{\Theta_0}(\lambda_1\lambda_2 - 1) - 3\alpha_0\kappa_0(\Theta - \Theta_0)(\lambda_1\lambda_2)^{\gamma - 1} = 0. \tag{49}$$

Note that eqn. (49) yields two solutions for λ_2 of different sign, so that the negative one must be always disregarded. Moreover, we note that λ_2 depends both on λ_1 and Θ. Employing now eqn. (24), the longitudinal stress can be obtained in the form

$$T_1 = \frac{\mu_0}{J}\frac{\Theta}{\Theta_0}\left(\lambda_1^2 - \lambda_2^2\right), \tag{50}$$

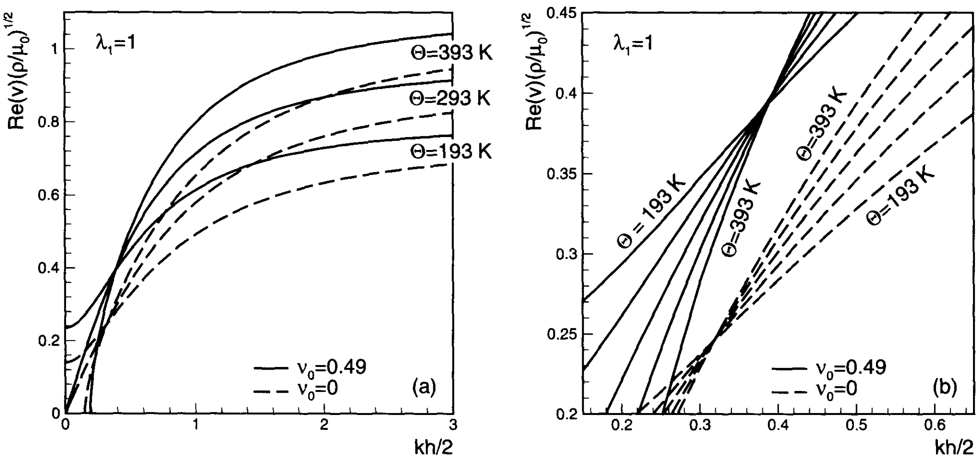

Figure 1. Dispersion diagrams for a single layer at different temperatures and for two values of Poisson ratio. Pre-strain is null, $\lambda_1 = 1$, and only results pertaining to the first mode of propagation are shown. Part (b) is a detail of part (a), in which additional values of temperature have been considered, $\Theta = \{193,\ 243,\ 293,\ 343,\ 393\}$ K.

representing the pre-stress state. It is immediate to observe from (50) that the pre-stress is positive (negative) when $\lambda_1 > \lambda_2$ ($<$). Therefore, the sign of the pre-stress depends through λ_2 on temperature and longitudinal stretch. In all the examples presented below the temperature sets the sign of the pre-stress when $\lambda_1 = 1$, whereas when $\lambda_1 = 1.3$ ($= 0.8$) the pre-stress remains tensile (compressive) for the whole range of temperature analyzed.

In the examples we systematically explore the condition of assigned wavenumber k, which is consequently taken to be real. Obviously, the frequency $\omega = kv$ turns out to be complex. This is related to the well-known fact that waves in thermoelastic materials are always dispersive, even in the cases of propagation of body and Rayleigh disturbances [22].

We have referred in all examples to the following values of parameters

$$\gamma = 2.5, \quad \alpha_0 = 10^{-4}\,\mathrm{K}^{-1}, \quad \Theta_0 = 293\,\mathrm{K}, \quad c = 1.8 \cdot 10^6\,\frac{\mathrm{N}}{\mathrm{m}^2\mathrm{K}}, \quad K = 0.2\,\frac{\mathrm{W}}{\mathrm{m\,K}},$$

and we have employed the Poisson ratio ν_0 defined in the unstressed configuration and at $\Theta = \Theta_0$, which is related to the elastic constants λ_0 and μ_0 through the well-known relationships

$$\nu_0 = \frac{\lambda_0}{2(\lambda_0 + \mu_0)}, \quad \lambda_0 = \frac{2\,\nu_0\,\mu_0}{1 - 2\,\nu_0}.$$

4.1. Single layer

Results for a single layer are reported in Figs. 1-2, where the phase velocity $\mathrm{Re}(v)$ – nondimensionalized through multiplication by $\sqrt{\rho/\mu_0}$ – is plotted versus the nondimensonal

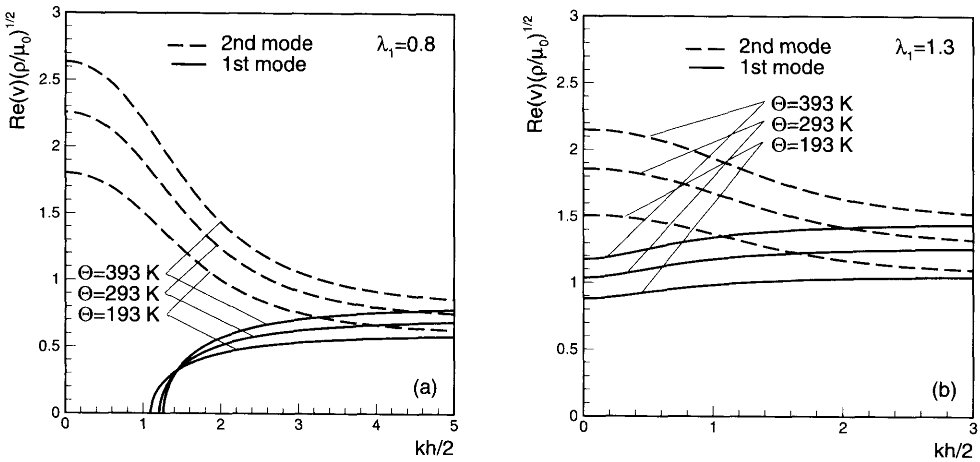

Figure 2. Dispersion diagrams for a single layer at different temperatures. Results pertaining to the first and second propagation mode are shown. Two values of longitudinal stretch are investigated, $\lambda_1 = 0.8$ corresponding to uniaxial compression, part (a), and $\lambda_1 = 1.3$ corresponding to uniaxial tension, part (b).

wave number $kh/2$, where h is the thickness of the layer. Three different values of temperature $\Theta = \{193, 293, 393\}$ K are considered for three values of λ_1, equal to 1 in Fig. 1, to 0.8 in Fig. 2(a), and to 1.3 in Fig. 2(b). The velocity corresponding to first and second mode of propagation are reported in Fig. 2, whereas only the slower propagation speeds are reported in all other figures.

Fig. 1 is relative to a null pre-strain, $\lambda_1 = 1$, so that the pre-stress is dictated by the temperature. Two extreme values of the Poisson ratio ν_0 are investigated in Fig. 1(a), namely, $\nu_0 = 0$ and $\nu_0 = 0.49$. It can be observed that the difference in ν_0 influences only quantitatively the results, but not qualitatively. Therefore, all subsequent results are restricted to the nearly incompressible case, $\nu_0 = 0.49$. A detail of Fig. 1(a) is reported in Fig. 1(b), where additional curves referring to five values of temperature, $\Theta = \{193, 243, 293, 343, 393\}$ K, have been added to highlight an interesting feature. In particular, while the phase velocity decreases with temperature at very low wave numbers, an opposite situation occurs for high wave numbers. A peculiar feature is that all curves intersect in a well definite point, within the numerical approximation. An effect of a tensile pre-stress is that it makes this point disappear from the graph, so that the wave speed always decrease with increasing temperature, see Fig. 2(b). The point of intersection of the curves in Fig. 1 corresponds to *a frequency and velocity of propagation which is independent of the temperature.*

Points in the graphs corresponding to a null velocity represent bifurcation conditions in a beam-like buckling mode. It is clear for $\lambda_1 = 1$, i.e. from Fig. 1(a), that an increase in temperature, which induces a compressive pre-stress, promotes bifurcation, whereas the occurrence of buckling may be eliminated by a decrease in temperature. This behaviour is also obviously influenced by the value of current stretch, which strongly modifies the state of pre-stress, see Fig. 2.

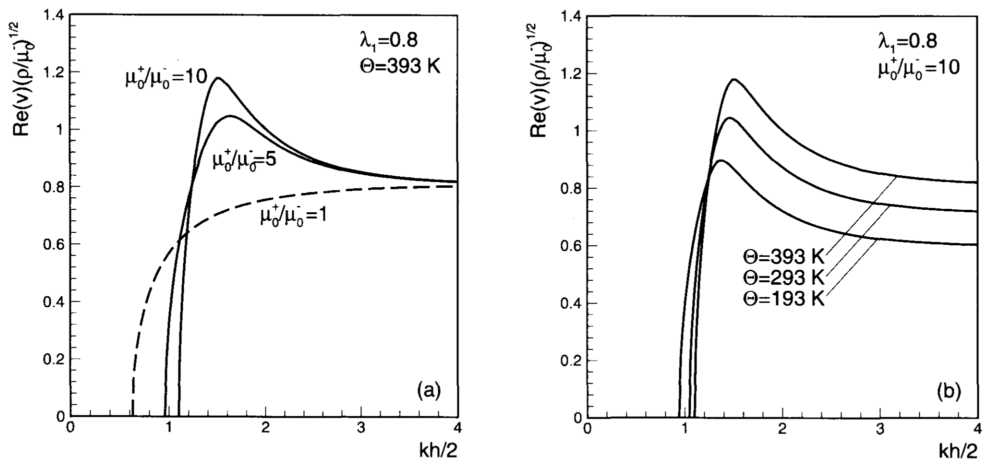

Figure 3. Dispersion diagrams for a two-layer structure, with $\lambda_1 = 0.8$, corresponding to a compressive pre-stress. The thickness of both layers is equal to h. Different values of stiffness ratios are investigated in part (a), whereas different temperatures are analyzed in part (b).

It should be finally noticed that results not reported for conciseness show that for sufficiently high values of the wavenumber k, the velocities become approximately equal to the values corresponding to Rayleigh waves.

4.2. Some simple layered geometries

Two layers of equal current thickness h are considered in Figs. 3–5. The layers differ only for the elastic stiffness μ_0, while all other parameters have been kept uniform, included the Poisson ratio, $\nu_0 = 0.49$, the thermal expansion coefficient, the conductivity and the heat capacity. The two layers have been labelled with superscripts $-$ and $+$, so that the two stiffnesses are denoted by μ_0^- and μ_0^+. In all figures, the phase velocity $\mathrm{Re}(v)$ is multiplied by $\sqrt{\rho/\mu_0^-}$ and plotted versus the nondimensional wave number $kh/2$.

Fig. 3 pertains to a compressive uniaxial pre-stress (for all investigated values of temperature), with a longitudinal stretch $\lambda_1 = 0.8$, whereas the pre-stress is tensile in Fig. 5, with $\lambda_1 = 1.3$. The pre-strain is null in Fig. 4, $\lambda_1 = 1$, so that the pre-stress only depends on temperature. Three different values of ratios between elastic moduli of the two layers, $\mu_0^+/\mu_0^- = \{1,\ 5,\ 10\}$, are considered in parts (a) for $\Theta = 393$ K, whereas $\mu_0^+/\mu_0^- = 10$ in parts (b), where temperature is varied, $\Theta = \{193,\ 293,\ 393\}$ K. Obviously, when the ratio between stiffnesses equals unity, $\mu_0^+/\mu_0^- = 1$, the two layers behave as a single layer of thickness $2h$, so that the curve is reported only for comparison. It appears clearly from Figs. 3–5 that temperature has a quantitative effect on the graphs, but not qualitative, whereas changing the stiffness ratio of the structure yields a strong, qualitative effect. An interesting feature of the results is that when the stiffness ratio increases, the curves evidence a peak so that propagation velocities initially increase at increasing wavenumber, but then a maximum is reached and speeds become decreasing functions of wavenumber.

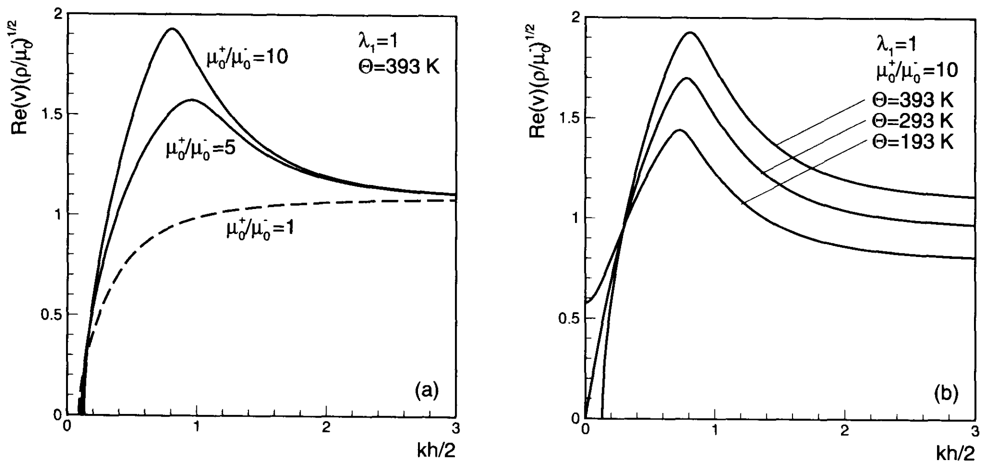

Figure 4. Dispersion diagrams for a two-layer structure, with $\lambda_1 = 1$, so that the pre-stress depends only on temperature. The thickness of both layers is equal to h. Different values of stiffness ratios are investigated in part (a), whereas different temperatures are analyzed in part (b).

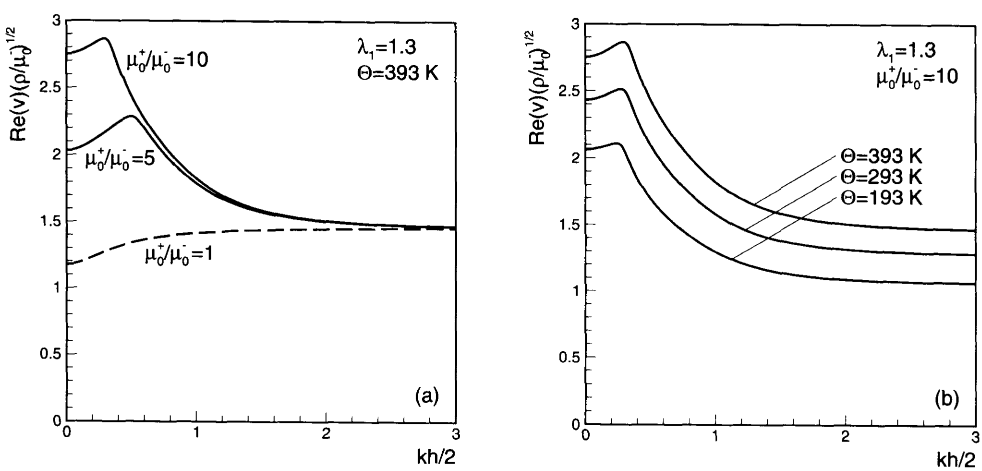

Figure 5. Dispersion diagrams for a two-layer structure, with $\lambda_1 = 1.3$, corresponding to a tensile pre-stress. The thickness of both layers is equal to h. Different values of stiffness ratios are investigated in part (a), whereas different temperatures are analyzed in part (b).

As a final example, we show in Fig. 6 results relative to a sandwich structure made up of three layers: two stiff and thin external coatings (denoted by superscript $-$) bonding a soft and thick internal core (denoted by superscript $+$). In particular, the current value of the thickness of the internal layer is five times greater than the thickness – denoted by h – of the two, identical, external layers. A state of compressive pre-stress has been considered, with

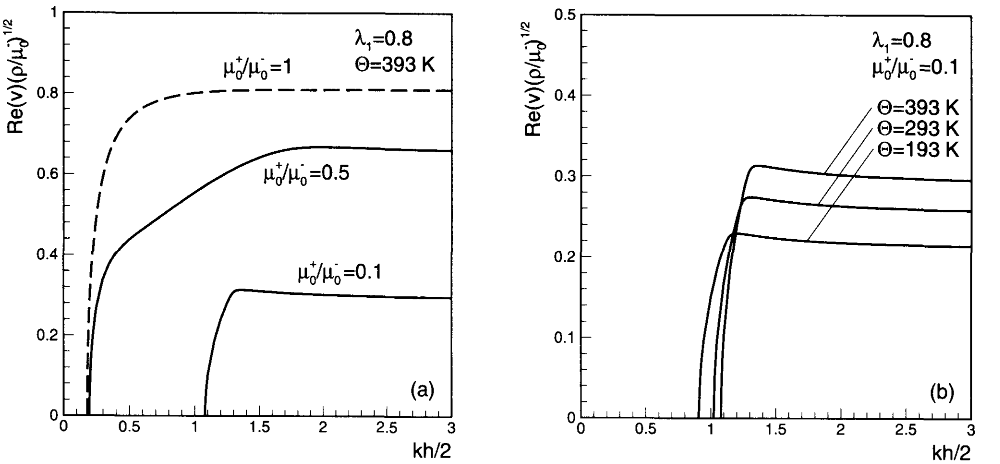

Figure 6. Dispersion diagrams for a three-layer structure, with $\lambda_1 = 0.8$, corresponding to a compressive pre-stress. The thicknesses of the external layers (labelled –) and core (labelled +) are h and $5h$, respectively. Different values of stiffness ratios are investigated in part (a), whereas different temperatures are analyzed in part (b).

$\lambda_1 = 0.8$ and two stiffness ratios $\mu_0^+/\mu_0^- = \{0.1,\ 0.5\}$ have been investigated, whereas all other parameters have been taken uniform.

Values pertaining to $\Theta = 393$ K are presented in Fig. 6(a), where $\mu_0^+/\mu_0^- = \{0.1,\ 0.5,\ 1\}$. Results relative to $\mu_0^+/\mu_0^- = 1$, represent a homogeneous single layer of thickness $7h$ and are reported for comparison (dashed curve). The effect of temperature is considered in Fig. 6(b), where $\Theta = \{193,\ 293,\ 393\}$ K.

It may be noted from Fig. 6(a) that the curve relative to $\mu_0^+/\mu_0^- = 0.1$ can be divided in two portions. In the initial portion, a small change in wavenumber is associated with a strong variation of the phase velocity, while, beyond the value $kh/2 \approx 1.35$, the phase velocity becomes almost independent of the wavenumber, revealing that the propagation mode is essentially a surface mode. The curve relative to $\mu_0^+/\mu_0^- = 0.5$ displays also two portions similar to those just mentioned, however these are separated by a transition zone where the change in velocity becomes almost proportional to the variation of the wavenumber.

It may be important to note that the bifurcation (corresponding to a null propagation velocity) is particularly enhanced by the soft core. In particluar, for the cosidered value of pre-strain $\lambda_1 = 0.8$ and for the stiffness ratio $\mu_0^+/\mu_0^- = 0.1$, a bifurcation occurs (when $kh/2 \leq 1.07$) in a mode which does not correspond to a beam-like, but to a surface instability. Fig. 6(b) shows that this effect results to be almost independent of the temperature.

5. CONCLUDING REMARKS

A general scheme has been given to analyze thermoelastic, small-amplitude waves superimposed upon a given homogeneous state of temperature and deformation in a multilaminated structure. In particular, elastic layers perfectly bonded to each other and deformed in plane strain have been considered, in a fully coupled theory of thermoelasticity. Results pertaining to a certain set of parameters show that the coupling, which makes the waves always dispersive, introduces only a weak effect, in the sense that the imaginary part of the propagation velocity turns out to be small, when compared to the real part. However, the temperature plays a strong quantitative role and may compensate effects related to pre-strain or different layer stiffness. Within a range of parameters, including the case of null pre-strain, results demonstrate that a particular value of frequency exists such that the propagation speed becomes independent of the temperature. This feature results to be strongly conditioned by the presence of pre-stress.

Acknowledgments. The Research Project MIUR-COFIN 2003 "Fenomeni di degrado meccanico di interfacce in sistemi strutturali: applicazioni in Ingegneria Civile ed a campi di ricerca emergenti" is gratefully acknowledged.

REFERENCES

[1] Hsueh, C.-H. and Ferber, M.K.: Apparent coefficient of thermal expansion and residual stresses in multilayer capacitors. *Composites Part A: Applied Science and Manufacturing* 33, 1115-1121 (2002).

[2] Icardi, U.: Free vibration of composite beams featuring interlaminar bonding imperfections and exposed to thermomechanical loading. *Composite Structures* 46, 229–243 (1999).

[3] Librescu, L. and Lin, W.: Vibration of thermomechanically loaded flat and curved panels taking into account geometric imperfections and tangential edge restraints. *Int. J. Solids Structures* 34, 2161–2181 (1997).

[4] Rutgerson, S.E. and Bottega, W.J.: Thermo-elastic buckling of layered shell segments. *Int. J. Solids Structures* 39, 4867–4887 (2002).

[5] Xu, K., Noor, A.K. and Tang, Y.Y.: Three-dimensional solutions for free vibrations of initially-stressed thermoelectroelastic multilayered plates. *Comput. Meth. Appl. Mech. Engrg.* 141, 125–139 (1997).

[6] Biot, M.A.: *Mechanics of Incremental Deformations*, John Wiley and Sons, New York, 1965.

[7] Steif, P.F.: Interfacial instabilities in an unbounded layered solid. *Int. J. Solids Structures* 26, 915–925 (1990).

[8] Triantafyllidis, N. and Leroy, Y.M.: Stability of a frictional material layer resting on a viscous half-space. *J. Mech. Phys. Solids* 42, 51–110 (1994).

[9] Steigmann, D.J. and Ogden, R.W.: Plane deformations of elastic solids with intrinsic boundary elasticity. *Proc. R. Soc. Lond.* A 453, 853–877 (1997).

[10] Bigoni, D., Ortiz, M. and Needleman, A.: Effect of interfacial compliance on bifurcation of a layer bonded to a substrate. *Int. J. Solids Structures* 34, 4305–4326 (1997).

[11] Bigoni, D. and Gei, M.: Bifurcations of a coated, elastic cylinder. *Int. J. Solids Structures* 38, 5117–5148 (2001).

[12] Dowaikh, M.A. and Ogden, R.W.: On surface waves and deformations in a pre-stressed incompressible elastic solids. *IMA J. Appl. Math.* 44, 261–284 (1990).

[13] Dowaikh, M.A. and Ogden, R.W.: Interfacial waves and deformations in pre-stressed elastic media. *Proc. R. Soc. Lond.* A 443, 313–328 (1991).

[14] Ogden, R.W. and Sotiropulos, D.A.: On interfacial waves in pre-stressed layered incompressible elastic solid. *Proc. R. Soc. Lond.* A 450, 319–341 (1995).

[15] Carlson, D.E.: Linear thermoelasticity. In *Mechanics of Solids*, Truesdell, C. (Ed.), Vol. II, Springer-Verlag, Berlin, pp. 297–345 (1972).

[16] Ogden, R.W.: On the thermoelastic modeling of rubberlike solids. *J. Thermal Stresses* 15, 533–557 (1992).

[17] Chadwick, P.: Thermo-mechanics of rubberlike materials. *Phil. Trans. Royal Soc. Lond.* A276, 371–403 (1974).

[18] Chadwick, P. and Creasy, C.F.M.: Modified entropic elasticity of rubberlike materials. *J. Mech. Phys. Solids* 32, 337–357 (1984).

[19] Roxburgh, D.G. and Ogden, R.W.: Stability and vibration of pre-stressed compressible elastic plates. *Int. J. Eng. Sci.* 32, 427–454 (1994).

[20] Ogden, R.W.: *Non-linear elastic deformations*, Ellis Horwood, Chichester, 1984.

[21] Flavin, J.N.: Thermo-elastic Rayleigh waves in a prestressed medium. *Proc. Camb. Phil. Soc.* 58, 532–538 (1962).

[22] Chadwick, P.: Thermoelasticity. The dynamical theory. In *Progress in Solid Mechanics* Sneddon, I.N. and Hill, R. (Eds.), North-Holland, Amsterdam, pp. 265–328 (1964).